(4) (a) Antonietti, M.; Coutandin, J.; Grütter, R.; Sillescu, H. *Macromolecules* **1984**, *17*, 798. (b) Antonietti, M.; Coutandin, J.; Sillescu, H. *Macromolecules* **1986**, *19*, 793.
(5) (a) Smith, B. A. *Macromolecules* **1982**, *15*, 469. (b) Smith, B. A.; Samulski, E. T.; Yu, L.-P.; Winnik, M. A. *Macromolecules* **1985**, *18*, 1901. (c) Smith, B. A.; Mumby, S. J.; Samulski, E. T.; Yu, L.-P. *Macromolecules* **1986**, *19*, 470.
(6) (a) Green, P. F.; Mills, P. J.; Palmstrom, C. J.; Mayer, J. W.; Kramer, E. J. *Phys. Rev. Lett.* **1984**, *57*, 2145. (b) Green, P. F.; Kramer, E. J. *Macromolecules* **1986**, *19*, 1108.
(7) Fleisher, G. *Polym. Bull.* **1984**, *11*, 75.
(8) Pearson, D. S.; Verstrate, G.; von Meerwall, E. D.; Schilling, F. G. *Macromolecules* **1987**, *20*, 1133.
(9) Watanabe, H.; Kotaka, T. *Macromolecules* **1987**, *20*, 530.
(10) Kim, H.; Chang, T.; Yohanan, J. M.; Wang, L.; Yu, H. *Macromolecules* **1986**, *19*, 2737.
(11) Ferry, J. D. *Viscoelastic Properties of Polymers*, 3rd ed.; John, Wiley: New York, 1980.
(12) Osaki, K.; Nishimura, Y.; Kurata, M. *Macromolecules* **1985**, *18*, 1153.
(13) Osaki, K.; Takatori, E.; Tsunashima, Y.; Kurata, M. *Macromolecules* **1987**, *20*, 525.
(14) Inoue, T.; Nemoto, N.; Kojima, T.; Kurata, M. *J. Soc. Rheol. Jpn.* **1988**, *16*, 72 (in Japanese); *Polym. J.* **1988**, *20*, 869.
(15) Inoue, T. Ph.D. Thesis, Kyoto University, 1988 (in Japanese).
(16) Deschamps, H.; Leger, L. *Macromolecules* **1986**, *19*, 2760.
(17) Doi, M.; Edwards, S. F. *J. Chem. Soc., Faraday Trans. 2* **1978**,*74*, 1789.
(18) In tracer diffusion, an extra degree of freedom associated with chain ends, is considered as an intrinsic property of the probe chain.
(19) de Gennes, P.-G. *Scaling Concepts in Polymer Physics*; Cornell University Press: Ithaca, NY, 1979.
(20) Nemoto, N.; Okada, S.; Inoue, T.; Kurata, M. *Macromolecules* **1988**, *21*, 1502.
(21) Nemoto, N.; Makita, Y.; Tsunashima, Y.; Kurata, M. *Macromolecules* **1984**, *17*, 2629.
(22) Nemoto, N.; Kojima, T.; Inoue, T.; Kurata, M. *Polym. J.* **1988**, *20*, 875.
(23) Callaghan, P. T.; Pinder, D. N. *Macromolecules* **1984**, *17*, 431.
(24) Marmonier, M. F.; Leger, L. *Phys. Rev. Lett.* **1985**, *55*, 1078.
(25) von Meerwall, E. D.; Amis, E. J.; Ferry, J. D. *Macromolecules* **1985**, *18*, 260.
(26) Numasawa, N.; Kuwamoto, K.; Nose, T. *Macromolecules* **1986**, *19*, 2593.
(27) Nemoto, N.; Landry, M. R.; Noh, I.; Kitano, T.; Wesson, J. A.; Yu, H. *Macromolecules* **1985**, *18*, 308.
(28) Wesson, J. A.; Noh, I.; Kitano, T.; Yu, H. *Macromolecules* **1984**, *17*, 431.
(29) Wheeler, L. M.; Lodge, T. P.; Hanleg, B.; Tirrell, M. *Macromolecules* **1987**, *20*, 1120.
(30) Philles, G. D. *Macromolecules* **1988**, *21*, 3101.
(31) Wheeler, L. M.; Lodge, T. P. *Macromolecules* **1989**, *22*, 2379.

Molecular Dynamics Simulation of the Condis State of Polyethylene†

D. W. Noid,* B. G. Sumpter,* and B. Wunderlich*

Chemistry Division, Oak Ridge National Laboratory, Oak Ridge, Tennessee 37831-6182, and Department of Chemistry, The University of Tennessee, Knoxville, Tennessee 37996-1600.
Received April 7, 1989; Revised Manuscript Received June 6, 1989

ABSTRACT: Using a realistic model for polyethylene (PE), the molecular dynamics technique is used to simulate atomic motion in a crystal. The calculations reveal conformational disorder above a critical temperature. The customarily assumed rotational isomers model is found to be a poor description of the crystal at elevated temperature. The rate of isomerization computed from molecular dynamics is compared to transition-state theory and leads to an activation energy of 23 kJ/mol, 6.3 kJ/mol above the single-bond rotation value. Classical heat capacities have been calculated and result in negative and positive deviations from $3R$, as was also observed experimentally. The negative expansion coefficient of the fiber axis is in good agreement with the experiment. A movie of the dynamics of the polyethylene crystal has been produced.

I. Introduction

In the study of crystals of flexible macromolecules, it has been demonstrated that a distinctly different type of mesophase with dynamic, conformational disorder can exist, the condis crystal.[1,2] Important ramifications of this conformational flexibility of PE chains on physical properties should include mechanical and dielectric relaxation, transport properties, and spectroscopy. Conformational disorder in isolated chains has been studied for many years using the Monte Carlo methods with the rotational isomeric model[3-5] in which the torsional angle, τ, is allowed to have only discrete values of 0 or $\pm 120°$. Recently, Yamamoto has used a continuous rotational model to study chain conformations in a crystal mean field.[6] One of the conclusions was that the rotational isomer model is not valid in a crystal environment. Several other studies have been made using molecular mechanics to understand the energetics of conformational disorder[7] and using normal mode theory[8] to clarify the effect of various conformational defects on infrared transitions.[9] Because these types of distortions or defects involve large-amplitude motion, which is anharmonic, it is not clear why the harmonic approximation (normal-coordinate analysis) would be valid and provide reliable results.

The purpose of this paper is to recognize the fact that conformational disorder in a polymer environment is a dynamic process and involves anharmonic motion. For this reason, we have used the molecular dynamics method (MD) to simulate conformational disorder more realisti-

† Research sponsored by the Division of Materials Sciences, Office of Basic Energy Sciences, U.S. Department of Energy, under Contract DE-AC05-840R21400 with Martin Marietta Energy Systems, Inc., and the National Science Foundation, Polymers Program, Grant No. 8818412.

0024-9297/90/2223-0664$02.50/0

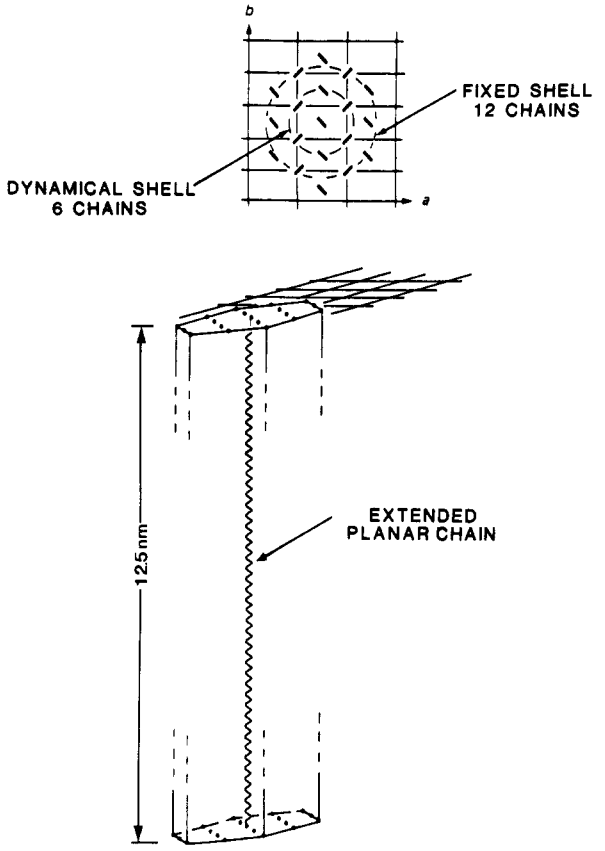

Figure 1. Diagram showing a region of a polyethylene crystal with 7 dynamic chains and 12 static chains.

Table I
Potential Energy Parameters

Two-Body Bonded Constants
D = 334.75 kJ/mol
r_e = 0.153 nm
γ = 19.9 nm^{-1}
Three-Body Bonded Constants
K_3 = 130.122 kJ/mol
cos θ_o = cos 113° = 0.3907 rad
K_{3A} = 331.37 kJ/mol·rad^2
O_{oA} = 113°
Two-Body Nonbonded Constants
ϵ = 0.4937 kJ/mol
σ = 0.4335 nm
Four-Body Bonded Constants
α = −18.4096 kJ/mol
β = 26.78 kJ/mol

cally. The MD method is, in addition, not only capable of providing the same type of information as generated from Monte Carlo simulations and molecular mechanics and normal-mode calculations but can also demonstrate transition behavior associated with phase changes. The MD method makes *no* assumptions about harmonic or collective motion and is the only practical way to probe time and temperature behavior in these large, nonlinear, and nonseparable systems. A careful implementation of the MD method for these systems is also capable of distinguishing between quasiperiodic and chaotic behavior in these systems.[10]

In the next section we present the necessary information about the implementation of molecular dynamics with our model of a polyethylene crystal. Various results of our calculations relating to the condis state and phase transition are described in section III, followed by conclusions in section IV.

II. Molecular Dynamics Method and Model

Our model for a polyethylene crystal includes seven dynamic chains surrounded by a shell of 12 fixed chains. A diagram of this 19-chain model is shown in Figure 1. This model is similar to the one recently used by Reneker and Mazur[8] to study the motion of defects except that our chain is longer and the end groups are not constrained. The extended chains in our crystal consist of 100 CH_2 groups each with a crystal thickness of ~12.6 nm. The Hamiltonian used for the molecular dynamics calculation is

$$H = \sum_{ic=1}^{7}\Bigg[\sum_{i=100(ic-1)+1}^{100ic}\frac{px_i^2 + py_i^2 + pz_i^2}{2M} + \sum_{i=100(ic-1)+1}^{(100)ic-1} V_{2bond}(r_{i,i+1}) + \sum_{i=100(ic-1)+1}^{100ic-2} V_3(\theta_{i,i+1,i+2}) + \sum_{i=100(ic-1)+1}^{100ic-3} V_4(\tau_{i,i+1,i+2,i+3})\Bigg] + \underbrace{V_{2NB}(R_{i,j})}_{\substack{\text{nonbonded}\\ \text{dynamical}\\ \text{chain interaction}}} + \underbrace{V_{2NB}(R_{i,k})}_{\substack{\text{nonbonded}\\ \text{dynamical-static}\\ \text{chain interactions}}}$$

This Hamiltonian represents the kinetic energy part in Cartesian momenta of particle i = 1–100 and consists of seven chains labeled ic = 1–7. For our calculations, we have collapsed the CH_2 groups into a single particle of mass 14. The potential energy functions are written in terms of two-body, three-body, and four-body bonded interactions (i.e., V_2, V_3, and V_4) and an additional nonbonded two-body term labeled V_{2NB}. The two-body potential term was fitted by Boyd[11] and is a Morse oscillator function with the form

$$V_2(r) = D(1 - e^{-\gamma(r-r_e)})^2$$

where r is the intermolecular distance and D, γ, and r_e are constants shown in Table I. The three-body term is

$$V_3(\theta) = \frac{1}{2}K_\theta(\cos\theta_o - \cos\theta)^2$$

θ is the angle between bonded atoms i, j, and k. In order to study the effect of bond bending flexibility on the condis transition, we also consider an alternate, more rigid three-body potential[11]

$$V_{3A}(\theta) = \frac{1}{2}K_{\theta A}(\theta - \theta_o)^2$$

We have considered several four-body potential functions[11] of the form (in internal torsional coordinates) $V_4(\tau) = \alpha\cos\tau + \beta\cos^3\tau$. The nonbonded interactions consist of two terms, the nonbonded interaction between the dynamical chains ic = 1–7 and the second term containing all the interactions between the 7 dynamic chains and the shell of the 12 static chains. The nonbonded interactions between the dynamic atoms do not contain 1–2 and 1–3 interactions in the neighbor list. The form of all the nonbonded interactions is the Lennard-Jones 6–12 potential

$$V_{NB}(R) = 4\epsilon((\sigma/R)^{12} - (\sigma/R)^6)$$

All the constants in the potential energy terms are presented in Table I.

Hamilton's equations

$$\dot{q} = \partial H/\partial p \qquad \dot{p} = -\partial H/\partial q$$

were integrated in Cartesian coordinates using the vectorized version of the differential equation solver ODE.[13]

This program is a variable-order, variable-time step method for integration of differential equations to a given error. For our present simulations, the error parameter was set to $\sim 10^{-5}$. The tedious and time consuming evaluations of the derivatives of the internal coordinates were drastically reduced using our geometric statement function method described in ref 14. A typical simulation of 25 ps required 2 h of CPU time on the CRAY XMP at ORNL.

Initially, all seven dynamic chains were in an extended zigzag on lattice sites of the orthorhombic phase of PE with $a = 0.74$ nm, $b = 0.49$ nm, and $c = 0.26$ nm. A randomly chosen amount of kinetic energy was placed initially in each atom of the dynamic chain. In a very short time, the energy was distributed among kinetic and potential energy to generate a fairly constant temperature. The temperature was computed from the standard equation

$$\frac{3}{2}NkT = \mathrm{KE} = \sum_{ic=1}^{7}\sum_{i=100}^{100ic}\frac{P_i^2}{2M}$$

Generation of trajectories with a 25-ps duration and the various correlation functions and rotational isomeric transitions (which are discussed in the next section) were computed.

III. Results and Calculations

With the model discussed in the previous section we have computed trajectories for several initial momentum distributions of the polymer atoms, which serve to explore the dynamics of our system at several temperatures. The resulting trajectory (position and momentum of all of the atoms) for all times t between 0 and 25 ps in intervals of 0.1 ps is then determined for each set of initial conditions or temperatures. The actual time step used in solving Hamilton's equations is considerably smaller than 0.01 and will vary in time as the program ODE changes the order of the method and the size of the time step to maintain the desired accuracy of the trajectory. In order to illustrate the MD method, two time sequences are shown in Figures 2 and 3 for temperatures of ~ 80 and ~ 430 K, respectively, in the interval from 0 to 1 ps. The sequence of pictures shows the movement of the lower 40 atoms of the seven chains in the crystal. A complete movie of the motion in the crystal has been produced. The low-temperature motion of Figure 2 is much more stable than the highly chaotic motion[10] of Figure 3. We note that although the pictorial representation of the motion alone does not yield rigorous criteria for chaotic dynamics, since the two trajectories appear qualitatively different, it strongly suggests this distinction.

Further analysis of the trajectory can reveal how fast the system equilibrates for rotational isomerization. From the trajectory, which reaches an equilibrium temperature of 430 K, we have histogrammed the distribution function of $\rho(\cos\tau)$ vs $\cos\tau$ at three intervals of time in Figure 4. The plot (a) is for the interval 0–5 ps, (b) for 10–15 ps, and (c) for 20–25 ps. The curves in Figure 4 reveal that, after a few picoseconds, the distribution function reaches a stable value. The distribution function $\rho(\cos\tau)$ at time zero contains only trans conformations; however, a very short time later some of the gauche conformational states and all intermediates become populated with the majority of the conformations remaining trans at $\cos\tau$ close to -1. Plots of equilibrated $\rho(\cos\tau)$ vs $\cos\tau$ histograms are presented in Figure 5 for several temperatures. These functions were obtained from the final 5 ps for the MD simulations with temperatures ranging from 150 to 400 K. It is very apparent that a much larger fraction of states with large deviations from the trans angle is found at higher temperatures. It is of inter-

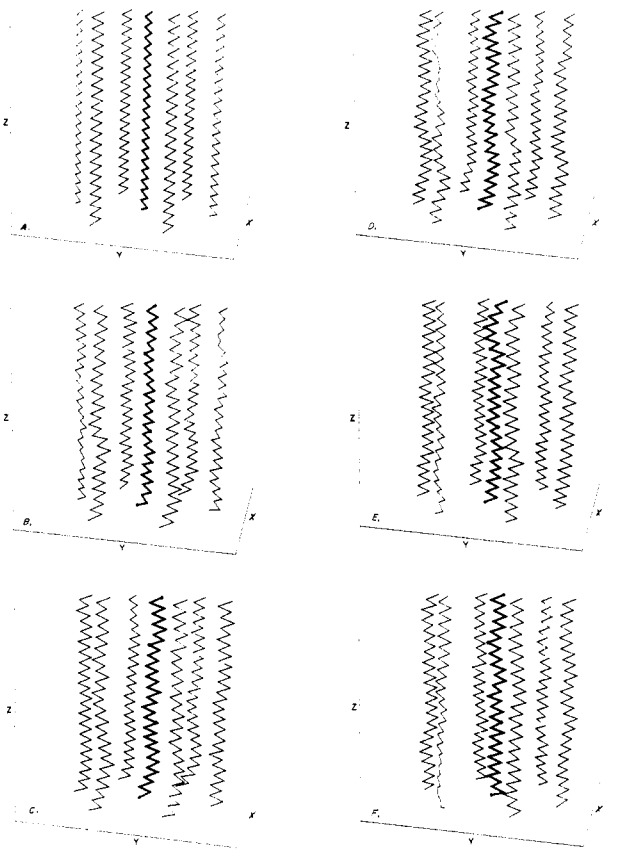

Figure 2. Movie sequence for values of $t = 0.1$, 0.3, 0.5, 0.7, and 0.9 ps for the low-temperature motion $T = 80$ K.

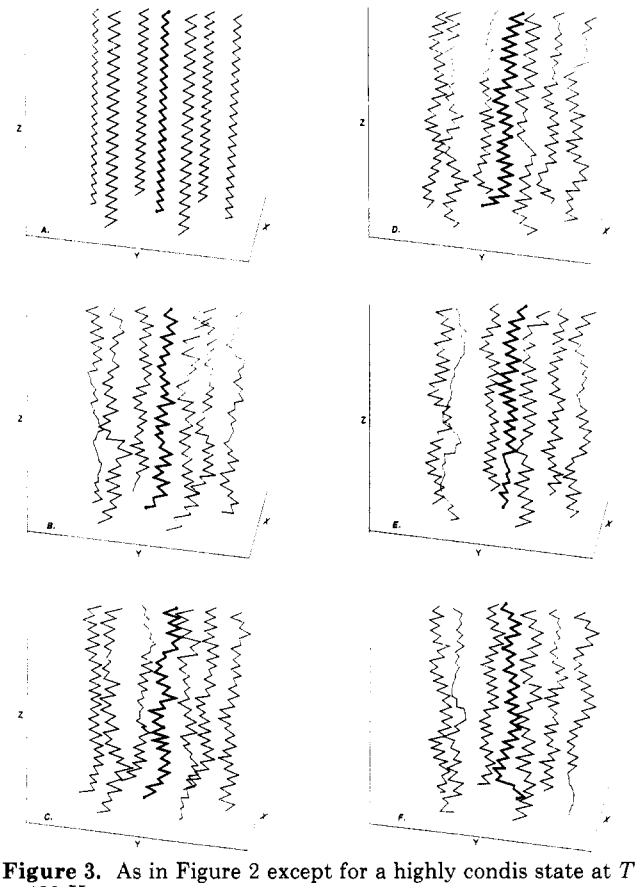

Figure 3. As in Figure 2 except for a highly condis state at $T = 430$ K.

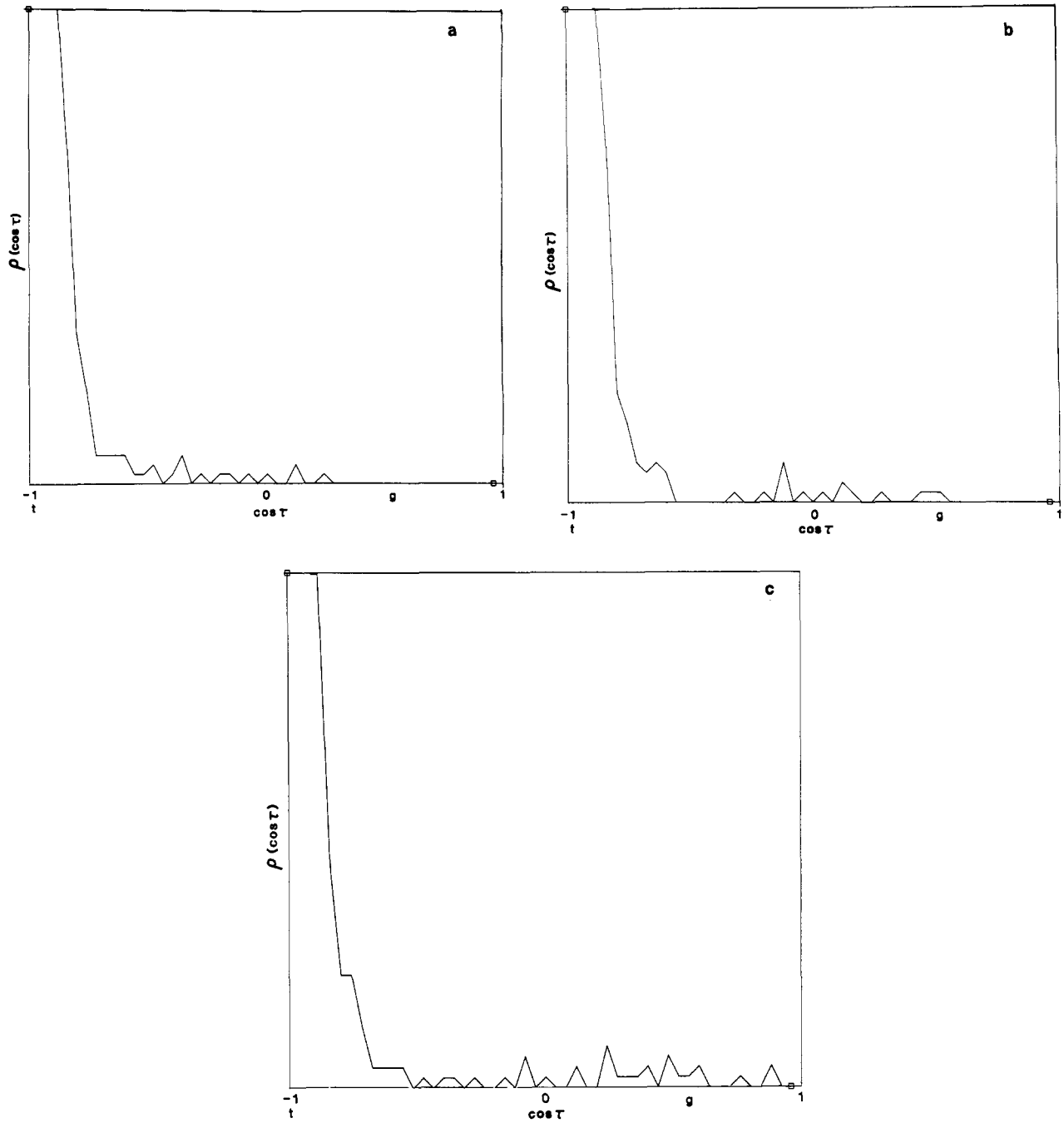

Figure 4. Plot of $\langle\rho(\cos\tau)\rangle$ vs cos τ for several time slices. Time t = 0–5, 10–15, and 20–25 ps of the trajectory with T = 430 are given in a–c, respectively.

est that there is no specific rotational isomer population accumulating outside of the low-energy trans conformer. This indicates that the rotational isomers model is not a valid description of the present simulation. Instead, once the trans isomer state is abandoned by a bond conformation, almost all intermediate states are populated.

A summary of all the results obtained from our simulation is found in Table II. The data in the columns temperature, T, total energy, ETOT, and end-to-end distance, R, were extracted from the final 20 ps of our 25-ps simulations. The results are averaged, and the variance is shown in the columns ΔT^2 and ΔR^2. The number of transitions were counted from the data each time the set of coordinates τ passed through 90° from trans. These data were analyzed for *new* transitions every 0.1 ps. The transition rate was then determined for the entire 25-ps simulation from transitions/25 ps. No transitions were observed at 149 K. The first conformational disorder is found between 149 and 228 K.

Transition-state theory for this isomerization yields a rate equation[15]

$$\text{rate} \equiv K_{\text{TST}} = N_{\text{ST}}\left(\frac{kT}{h}\right)e^{-E^*/kT}$$

where k, T, and h have the customary meanings and N_{ST} is a statistical factor and equals the number of torsional sites, i.e., 7 × 97. The values of E^* needed to match the data in Table II range from 20.50 to 25.52 kJ/mol with an average value of 23.012 kJ/mol. This is considerably higher than the barrier height of 16.74 kJ/mol for an isolated rotation. The additional energy of 6.3 kJ is needed to create a volume element for an isomeric transition to occur.

To test the importance of bond bending on our results,

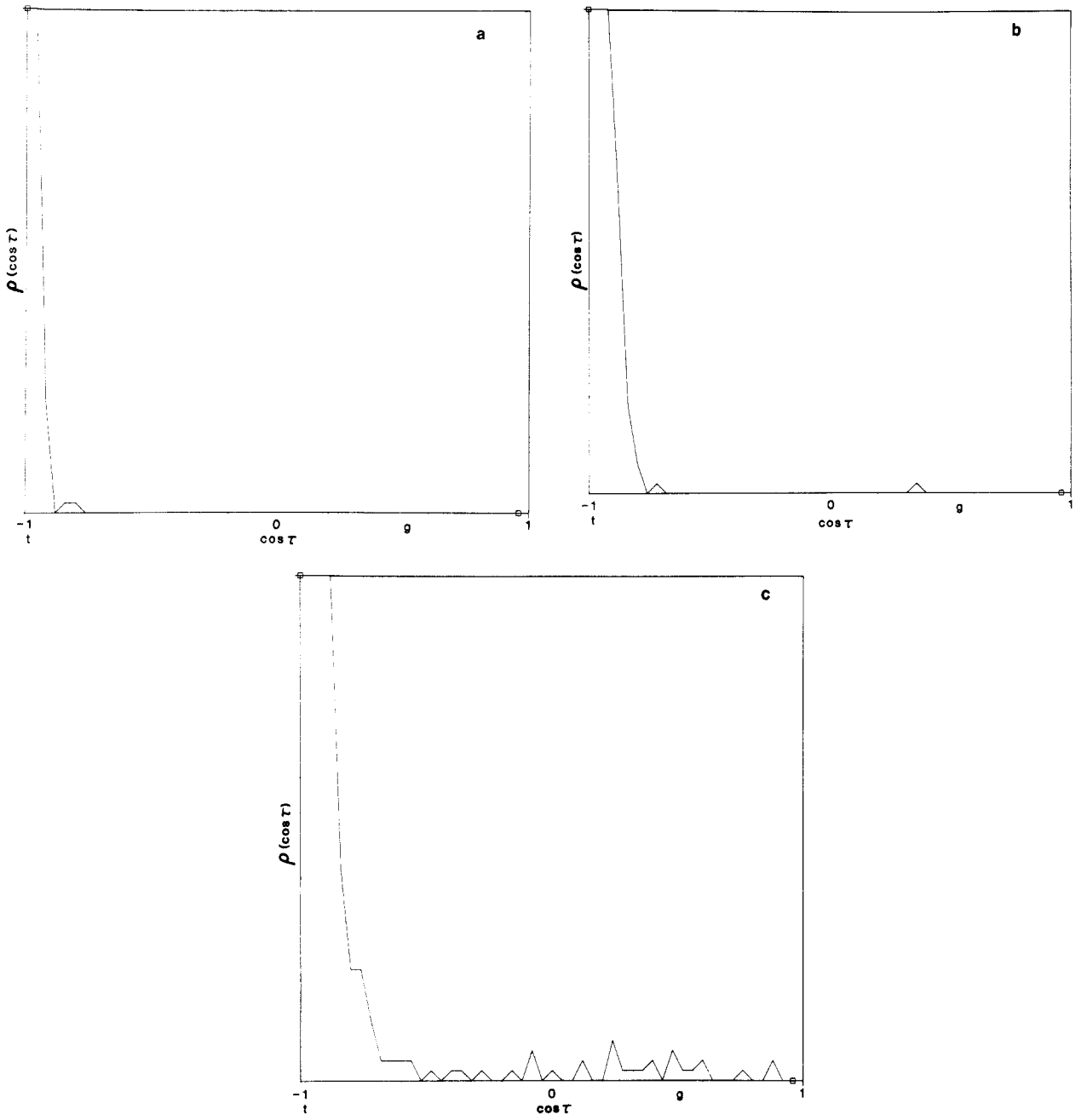

Figure 5. Plot of $\langle\rho(\cos\tau)\rangle$ vs $\cos\tau$ for the final 5 ps of the trajectory with T = 150, 320, and 400 K in parts a–c, respectively.

Table II
Results of MD Calculations

T, K	ΔT^2	ETOT, kJ/mol	R, nm	ΔR^2	transitions/25 ps[a]	transition rate	E^*,[b] kJ/mol	c
43.95	2.3×10^{-2}	-12305	12.636	2.35×10^{-4}	0	0		
148.96	9.5×10^{-2}	-10472	12.619	3.76×10^{-6}	0	0		$3.0R$
228.46	0.114	-9096	12.612	2.16×10^{12}	1 or 2	0.06×10^{12}	20.5	$2.975R$
324.4	0.102	-7401	12.603	1.88×10^{-3}	9	0.36×10^{12}	25.5	$3.036R$
397.21	1.93	-6046	12.558	6×10^{-4}	131	5.24×10^{12}	23.0	$3.199R$
433.14	0.006	-5406	12.572	6×10^{-3}	225	9.0×10^{12}	23.4	$3.060R$
538.76	1.505	-3121	12.508	4.5×10^{-3}	58*	58.0×10^{12}	21.7	$3.716R$

[a] Counted for 1 ps only. [b] Av E^* = 23.012 kJ/mol.

we also carried out a simulation with the different potential V_{3A} substituted for V_3 as given above. This potential leads to a considerably less flexible (elastic) chain. During the 25-ps trajectory at a temperature of 446 K, only 15 isomeric transitions were observed for a rate of 0.6×10^{12}. Similar results have been found for the melting transition of polyethylene.[16] Using the same equation for K_{TST}, we found $E^* \sim 38$ kJ/mol. This illustrates the need for using realistic potentials and including the proper bending mode in these simulations.

Other interesting results that can be extracted from the present simulation involve the shrinking of the PE crystal (change in fiber period) as indicated by the size of the central dynamic chain. The end-to-end distance R is reduced by approximately 0.3% upon heating to 324 K (about room temperature). This agrees well with the

experimental shrinking of the fiber period for PE.[17,18]

Finally, we have computed heat capacities and temperature fluctuations using the energy and temperature results. The heat capacity was computed from the relation $C = \Delta E/\Delta T$ where ΔT is the average temperature difference computed from the final 20 ps of the trajectories. Initially we find a heat capacity close to the expected classical $3R$ ($C = 2.999R$). At temperatures above 150 K, this heat capacity falls off a small amount as condis states are approached (because of the changes of vibrators to rotators). Then the heat capacity rises in the temperature range of 324–397 K as condis transitions to the higher energy condis states take place. In the range 433–539 K, another stronger increase in heat capacity is seen as the disorder increases more drastically. Perhaps this added increase indicates processes more like melting. Experimental heat capacities parallel this variation in heat capacity closely with a minimum at 250 K and an increase above 350 K.[19,20]

In order to fully simulate the condis and melt states and the transitions between the states, it will be necessary to relax the constant-volume restriction of our model (Figure 1). Further work in this direction is being planned.

IV. Conclusions

When the molecular dynamics method was used to model the motion of a polyethylene chain in a crystal environment, various encouraging results were found.

A transition to a conformational disordered crystal was observed. This is apparent from both the movie of our results (partially shown in Figures 2 and 3) and the calculations of the isomeric transition rates.

Although we have a fairly accurate simulation, no specific defect type or motion was readily apparent. There are several possible explanations for this.

(1) A special waveform may be needed for defect motion, and none was generated or created on our short time scale.

(2) The chosen potential energy function may still not model motion realistically.

(3) Chaotic motion becomes predominant at sufficiently low temperatures to damp out any collective modes necessary for a generation of soliton or a stable defect waveform.

Similar to the failure to detect specific defects, and probably linked to some degree, is the failure to observe the usually assumed more stable gauche conformations of the rotational isomeric states model.

Other positive aspects of this report include the correct trends in the crystal heat capacities and fiber period.

In future work we plan to extend the simulation to longer times and to add another dynamical shell to our crystal.

Acknowledgment. D.W.N. acknowledges helpful discussions with Professors S. Z. D. Cheng and D. Reneker in the earlier stages of this work.

Registry No. Polyethylene, 9002-88-4.

References and Notes

(1) Wunderlich, B.; Grebowicz, J. *Adv. Polym. Sci.* **1984**, *60/61*, 1.
(2) Wunderlich, B.; Möller, M.; Grebowicz, J.; Baur, H. *Conformational Disorder in Low and High Molecular Mass Crystals*; Springer-Verlag: Berlin, 1988; *Adv. Polym. Sci.* **1989**, *87*.
(3) Flory, P. J. *Structural Mechanics of Chain Molecules*; Wiley-Interscience: New York, 1969.
(4) Birshthein, T. M.; Ptitsyn, O. B. *Conformations of Macromolecules*; Wiley-Interscience: New York, 1966.
(5) Volkenstein, M. V. *Configurational Statistics of Polymeric Chains*; Wiley-Interscience: New York, 1963.
(6) Yamamoto, T. *Polymer* **1984**, *24*, 943. *Ibid.* **1984**, *25*, 178.
(7) Miller, K. J.; Grebowicz, J.; Wesson, J.; Wunderlich, B. *Macromolecules*, in press.
(8) Reneker, D. H.; Mazur, J. *Polymer* **1988**, *29*, 3. Reneker, D. H.; Mazur, J. Crystallographic Defects in Polymers and What They Do. *Polym. Prepr.*
(9) Zerbi, G.; Longhi, G. *Polymer* **1988**, *29*, 1827.
(10) For a chemical dynamics review of the chaos, see: Noid, D. W.; Koszykowski, M. L.; Marcus, R. A. *Ann. Phys. Chem.* **1981**, *32*, 267.
(11) Sorensen, R. A.; Liam, W. B.; Boyd, R. H. *Macromolecules* **1988**, *21*, 194. Boyd, R. H. *J. Chem. Phys.* **1968**, *49*, 2574.
(12) Weber, T. A. *J. Chem. Phys.* **1979**, *70*, 4277. *Ibid.* **1978**, *69*, 2347.
(13) Shampine, L. F.; Gordon, M. K. *Computer Solution of Ordinary Differential Equations: The Initial Value Problem*; Freeman: San Francisco, 1975.
(14) Noid, D. W.; Sumpter, B. G.; Wunderlich, B.; Pfeffer, G. A. *J. Comput. Chem.*, in press.
(15) See, for example: Elias, H. G. *Macromolecules*; Plenum Press: New York, 1984; Vol. 1, p 96.
(16) Sumpter, B. G.; Noid, D. W.; Wunderlich, B., to be submitted for publication.
(17) Davis, G. T.; Eby, R. K.; Colson, J. P. *J. Appl. Phys.* **1970**, *41*, 4316.
(18) Baughman, R. H. *J. Chem. Phys.* **1973**, *58*, 2976.
(19) Gaur, U.; Wunderlich, B. *J. Phys. Chem. Ref. Data* **1981**, *10*, 119.
(20) Pan, R.; Varma, M.; Wunderlich, B. *J. Therm. Anal.*, in press.